CANCER THERAPY

MEK inhibitor trametinib does not prevent the growth of anaplastic lymphoma kinase (ALK)–addicted neuroblastomas

Ganesh Umapathy,[1] Jikui Guan,[1] Dan E. Gustafsson,[1] Niloufar Javanmardi,[2] Diana Cervantes-Madrid,[1] Anna Djos,[2] Tommy Martinsson,[2] Ruth H. Palmer,[1] Bengt Hallberg[1]*

Activation of the RAS-RAF-MEK-ERK signaling pathway is implicated in driving the initiation and progression of multiple cancers. Several inhibitors targeting the RAS-MAPK pathway are clinically approved as single- or polyagent therapies for patients with specific types of cancer. One example is the MEK inhibitor trametinib, which is included as a rational polytherapy strategy for treating EML4-ALK–positive, EGFR-activated, or KRAS-mutant lung cancers and neuroblastomas that also contain activating mutations in the RAS-MAPK pathway. In addition, in neuroblastoma, a heterogeneous disease, relapse cases display an increased rate of mutations in *ALK*, *NRAS*, and *NF1*, leading to increased activation of RAS-MAPK signaling. Co-targeting ALK and the RAS-MAPK pathway is an attractive option, because monotherapies have not yet produced effective results in ALK-addicted neuroblastoma patients. We evaluated the response of neuroblastoma cell lines to MEK-ERK pathway inhibition by trametinib. In contrast to RAS-MAPK pathway-mutated neuroblastoma cell lines, ALK-addicted neuroblastoma cells treated with trametinib showed increased activation (inferred by phosphorylation) of the kinases AKT and ERK5. This feedback response was mediated by the mammalian target of rapamycin complex 2–associated protein SIN1, resulting in increased survival and proliferation that depended on AKT signaling. In xenografts in mice, trametinib inhibited the growth of EML4-ALK–positive non–small cell lung cancer and RAS-mutant neuroblastoma but not ALK-addicted neuroblastoma. Thus, our results advise against the seemingly rational option of using MEK inhibitors to treat ALK-addicted neuroblastoma.

INTRODUCTION

The mitogen-activated protein kinase (MAPK) kinase (MEK) protein kinase occupies a crucial signaling node downstream of RAS and RAF and directly upstream of extracellular signal–regulated kinase (ERK) and, hence, has been the subject of intensive drug discovery activities. Genetic and biochemical analyses of MEK function have suggested that MEK activity is necessary for the transforming and proliferative effects of this pathway, suggesting that therapeutics that completely inhibit MEK function may have utility in the treatment of cancers driven by activation of the RAS-RAF-MEK-MAPK axis. The MAPK signaling axis is involved in cancer initiation, maintenance, and resistance to therapy. MAPK activation often occurs through mutations and amplifications in upstream receptor tyrosine kinases (RTKs) (*ALK*, *EGFR*, and *ERBB2*), mutations in signal transduction genes (*NRAS* and *KRAS*), and/or pathway regulatory genes (*NF1* and *PTPN11*) (*1*).

MEK inhibitors, such as trametinib, suppress signaling through the MAPK cascade displaying anticancer activity and are approved as single agents for treatment of B-rapid accelerated fibrorsarcoma (BRAF)–positive melanoma (*2*–*4*). Recently, MEK inhibitors, such as trametinib, selumetinib, and binimetinib, have been included as a rational polytherapy strategy for treating EML4–ALK (anaplastic lymphoma kinase)–, EGFR (epidermal growth factor receptor)–, and KRAS-mutant lung cancer, as well as for naïve and relapsed high-risk neuroblastoma containing hyperactivating RAS-MAPK mutations (*5*–*13*). Here, we investigate the polytherapy hypothesis in ALK-positive neuroblastoma using trametinib and ALK inhibitors. Our aim was to address whether MEK inhibition alone or in combination has therapeutic value in neuroblastoma through evaluation of a large panel of neuroblastoma cell lines.

Neuroblastoma is derived from the neural crest of the postganglionic sympathetic nervous system and is a heterogeneous disease with a span from spontaneous regression to untreatable progression. New treatment approaches, including surgery, chemoradiotherapy, stem cell transplantation, and immunotherapy, have improved cure rates, but high-risk neuroblastoma patients are still challenging (*14*–*17*). Genetically, neuroblastoma is characterized by frequent deletion of parts of the chromosomes 1p and 11q, gain of parts of 17q, and/or *MYCN* gene amplification (*18*–*20*). The gene encoding the RTK ALK was identified as a neuroblastoma predisposition gene, and constitutive active mutations were found and verified to be active within the kinase domain in both germline and somatically acquired neuroblastomas (*21*–*25*). Moreover, the incidence of activating point mutations in *ALK* in relapsed neuroblastoma patients is ~20 to 43% (*8*, *26*–*28*). With this in mind, the rationale for combinatorial treatment of neuroblastoma is a well-grounded hypothesis given that previous preclinical combinations of tyrosine kinase inhibitors (TKIs) with other kinase inhibitors have shown good response in several cancer types (*6*, *29*–*33*).

Here, we investigated whether growth of neuroblastoma cell lines harboring a hyperactivated RAS-MAPK pathway is suppressed by the U.S. Food and Drug Administration–approved MEK inhibitor trametinib, either alone or as a partner in a combinatorial therapy approach. We found that EML4-ALK–positive lung cancer cells and RAS-MAPK pathway–mutated neuroblastoma cell lines are sensitive to MEK-targeted therapies; however, MEK inhibition is not beneficial in ALK-addicted neuroblastoma cells that have a hyperactivated RAS-MAPK pathway. Rather, in these ALK-addicted neuroblastoma cells, inhibition of MEK resulted in the phosphorylation of the mammalian

[1]Department of Medical Biochemistry and Cell Biology, Institute of Biomedicine, Sahlgrenska Academy, University of Gothenburg, SE-405 30 Göteborg, Sweden. [2]Department of Clinical Pathology and Genetics, Institute of Biomedicine, Sahlgrenska Academy, University of Gothenburg, SE-405 30 Göteborg, Sweden.
*Corresponding author. Email: bengt.hallberg@gu.se

target of rapamycin complex 2 (mTORC2) partner stress-activated protein kinase (SAPK)–interacting protein 1 (SIN1), resulting in increased survival and growth that are dependent on AKT signaling activity.

RESULTS

Neuroblastoma cell lines are differentially sensitive to the MEK inhibitor trametinib

Trametinib is a specific and potent MEK inhibitor with a median inhibitory concentration (IC_{50}) of about 1 to 2 nM in cell-free assays (*2*–*4*). Currently, trametinib is involved in several clinical trials (ClinicalTrials.gov) either as a single agent or as part of a combinatorial strategy. Trametinib has been suggested to be used with ALK inhibitors in a rational polytherapy strategy for neuroblastoma. This is a rational approach based on the robust activation of the RAS-MAPK pathway upon ALK receptor ligation. Thus, we set out to test this hypothesis experimentally. Because neuroblastoma is a heterogeneous disease, we first investigated the neuroblastoma cell lines used in this study by defining their characteristics and oncogenic drivers. All cell lines used were subjected to single-nucleotide polymorphism (SNP) analysis using Affymetrix CytoScan HD arrays and sequenced for mutations in *ALK*, *RAS*, and *p53*. Further, NF-1 and insulin-like growth factor 1 receptor/insulin receptor (IGFR/IR) abundance was investigated (figs. S1 and S2, Table 1, and table S1).

We first focused on the CLB-BAR, CLB-GE, CLB-GAR, and Kelly neuroblastoma cell lines, which have previously been shown to be ALK-addicted (Fig. 1) (*23*, *34*–*36*). The SK-N-AS and SK-N-BE cell lines have activating mutations in the *NRAS* gene and exhibit down-regulated *NF1* expression, respectively (Table 1 and fig. S1), leading to activation of the RAS-MAPK pathway (*37*). Additional neuroblastoma cell lines used were IMR32, whose growth can be suppressed by insulin-like growth factor receptor (IGFR) inhibitors (*38*), CLB-PE, which expresses mutant p53 (Table 1), and SK-N-DZ, which expresses mutant p53 (R110L) and has a high abundance of activated IGF receptors [see fig. S2B and the Cosmic database (http://cancer.sanger.ac.uk/cell_lines)] (*39*). Because these cell lines have not been sequenced at the whole-genome level, additional oncogenic drivers may exist (Table 1).

After genetic characterization, cell lines were treated with either the MEK inhibitor trametinib (10 nM) or the ALK inhibitor lorlatinib (30 nM). Proliferation was assessed for over 12 days. Proliferation of the RAS-activated neuroblastoma cell lines (SK-N-AS and SK-N-BE) was sensitive to trametinib treatment (Fig. 1, A and B). In contrast, ALK-positive neuroblastoma cell lines (CLB-BAR, CLB-GE, CLB-GAR, and Kelly) continued to grow upon trametinib treatment for at least 12 days (Fig. 1, A and B). Increasing the dose to 100 nM, 10 times its IC_{50} value, resulted in growth inhibition of all cell lines tested. In agreement with previous findings, all ALK-addicted neuroblastoma cells tested exhibited sensitivity to the ALK inhibitor lorlatinib (Fig. 1, A and B) (*36*, *40*). We also observed that neuroblastoma cell lines with mutations in p53, such as CLB-PE and SK-N-DZ, or high expression of IGF, similar to the IMR32 line, were insensitive to trametinib (Fig. 1B).

To further investigate the role of RAS-MEK-ERK signaling, the CLB-BAR and CLB-GE ALK-addicted neuroblastoma cell lines were treated with low nanomolar amounts of trametinib alone, lorlatinib alone, or a combination of both (Fig. 1, C and D). The combination of different concentrations of trametinib and lorlatinib did not result in synergistic inhibition of proliferation in ALK-positive neuroblastoma cell lines when compared to monotreatment (Fig. 1, C and D, and table S2). Thus, these results suggest that neuroblastoma cell lines

Table 1. Mutation data for the cell lines. Mutation data for selected critical genes for the nine neuroblastoma cell lines used in this study. MNA, MYCN-amplified; HomZ., homozygote; mut, mutant; amp, amplification; ex, exon; expr., expression.

Cell line	Genomic profile*	ALK status (amp, mut ex23–25)	MYCN status	TP53 status mut ex5–9	NRAS status	NF1 expr.
CLB-BAR	MNA	Amp. whole ALK exc. part of i3 (nonamp). Note, exome sequencing shows del ex4–11†	MYCN-amplified	No mut in TP53	No mut in NRAS	High
CLB-GE	MNA	ALK amp. ALK mut F1174V	MYCN-amplified	No mut in TP53	No mut in NRAS	High
CLB-GAR	11q-del	2p gain with break within ALK intron 1. Mutation R1275Q	Not MYCN-amplified	No mut in TP53	No mut in NRAS	High
Kelly	MNA + 11q-del	No amplification. 2p-gain. Mutation F1174L	MYCN-amplified	HomZ. Mut P177T	No mut in NRAS	High
SK-N-DZ	MNA	No mutation. No amplification	MYCN-amplified	No mut in TP53	No mut in NRAS	Intermediate
CLB-PE	MNA + 11q-del	2p gain. No mutation. No amplification	MYCN-amplified	HomZ. mut C176F	No mut in NRAS	High
IMR32	MNA	Amp. of ALK ex3–4 only. No mutation	MYCN-amplified	No mut in TP53	No mut in NRAS	High
SK-N-AS	11q-del	No mutation. No amplification	Not MYCN-amplified	No mut in TP53	Mut in NRAS: Q61K	Low
SK-N-BE	MNA	2p gain. No mutation. No amplification	MYCN-amplified	HomZ. mut C145F	No mut in NRAS	Low

*Genomic profile as defined in (*74*). †Genomic profile as defined in (*75*).

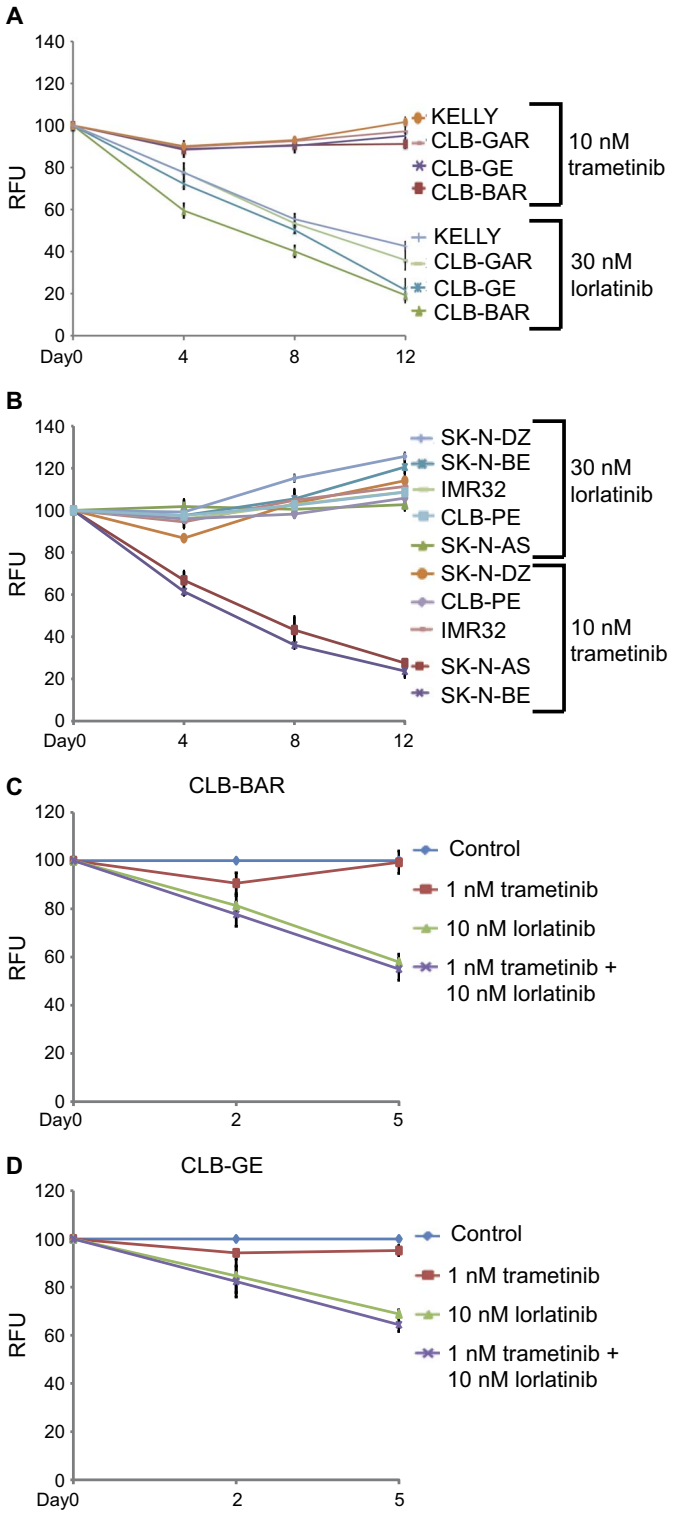

Fig. 1. Sensitivity of neuroblastoma cell lines to MEK inhibition by trametinib. (**A** and **B**) Viability assessed over 12 days using the resazurin viability assay in neuroblastoma cell lines [CLB-BAR, CLB-GE, CLB-GA, and Kelly in (A) and SK-N-AS, SK-N-BE, SK-N-DZ, IMR32, and CLB-PE in (B)] treated with either trametinib or lorlatinib, as indicated. (**C** and **D**) Resazurin assay–based viability in neuroblastoma cell lines CLB-BAR (C) and CLB-GE (D) treated with trametinib or lorlatinib alone or a combination of trametinib and lorlatinib, as indicated. Data are means ± SE of fold relative fluorescence units (RFU) relative to untreated cells from three independent experiments.

exhibiting ALK-addicted, high-IGFR, and *TP53*-mutated characteristics are not primarily dependent on RAS-MAPK pathway signaling for survival and proliferation, in contrast to those with direct RAS-MAPK pathway aberrations.

ALK-addicted neuroblastoma cell lines are dependent on the AKT pathway

We next set out to investigate the mechanisms underlying the lack of sensitivity of ALK-addicted neuroblastoma cell lines to MEK inhibition. Given that previous observations have indicated that the PI3K (phosphatidylinositol 3-kinase)–mTOR–ERK5 signaling complex is important for the survival of ALK-addicted neuroblastoma cells (*32*, *33*), we investigated the activity of the AKT-mTOR-ERK5 pathway in response to trametinib treatment. Upon treatment with trametinib, ALK-addicted cell lines exhibited a twofold increased phosphorylation (activation) of both AKT and ERK5 (Fig. 2, A to C). A similar increase in AKT activity was observed in the Kelly cell line (fig. S3A) and the p53-mutated cell lines SK-N-DZ and CLB-PE (fig. S3C) but not in the RAS-MAPK pathway–mutant cell lines SK-N-AS and SK-N-BE (fig. S3D). To further evaluate the dependence of AKT-ERK5 signaling, we treated CLB-GE and CLB-BAR with PI3K (BEZ235) and ERK5 (XMD8-92) inhibitors. Both PI3K and ERK5 inhibitors reduced the phosphorylation levels of AKT (at Ser^{473}) and ERK5 (at Thr^{218}/Tyr^{220}), respectively, but had no effect on the phosphorylation of MAPK (fig. S4A). Together, our data reveal the importance of the AKT signaling core in ALK-addicted neuroblastoma cells and that it is potentiated in response to MEK inhibition.

Activation of AKT downstream from ligand-activated ALK is enhanced upon treatment with trametinib

ALKAL1 (FAM150A and AUGβ) and ALKAL2 (FAM150B and AUGα) are potent ligands for ALK (*41*–*43*), prompting us to investigate the effect of trametinib inhibition on ALK signaling in response to ALKAL1 stimulation. We used the IMR32 neuroblastoma cell line, which harbors a ligand-responsive ALK in which exons 2 to 4 of ALK are amplified (Table 1). In agreement with our previous findings (*41*), we observed that stimulation of IMR32 cells with ALKAL1 led to the phosphorylation of both AKT (Ser^{473}) and ERK5 (Thr^{218}/Tyr^{220}) that was abrogated in the presence of the ALK inhibitor lorlatinib in combination with trametinib (Fig. 2D). Similar results were observed in the ALK-addicted cell line CLB-GE (fig. S4B). In contrast, in ALKAL1-stimulated IMR32 cells, inhibition of MEK with trametinib increased the phosphorylation of both AKT and ERK5 close to twofold and reduced the phosphorylation of ERK1/2. This increase in AKT and ERK5 phosphorylation was dependent on ALK activity because lorlatinib inhibited this response and treatment of IMR32 cells with trametinib alone showed no increase in either AKT or ERK5 phosphorylation (Fig. 2D). These results indicate that the activity of the ALK itself is important in the increased activation of AKT signaling core in response to trametinib.

We next tested whether this response was unique to ALK-addicted neuroblastoma cells by investigating the effect of trametinib on AKT signaling in the EML4-ALK–positive H3122 and DFCI032 non–small cell lung cancer (NSCLC) cell lines. Proliferation and AKT signaling were examined in both H3122 and DFCI032 cells after treatment with either trametinib or lorlatinib. In contrast to ALK-addicted neuroblastoma cells, we observed that (i) both EML4-ALK–positive H3122 and DFCI032 NSCLC cells were sensitive to trametinib and that (ii) the increased activation of AKT signaling seen upon trametinib treatment

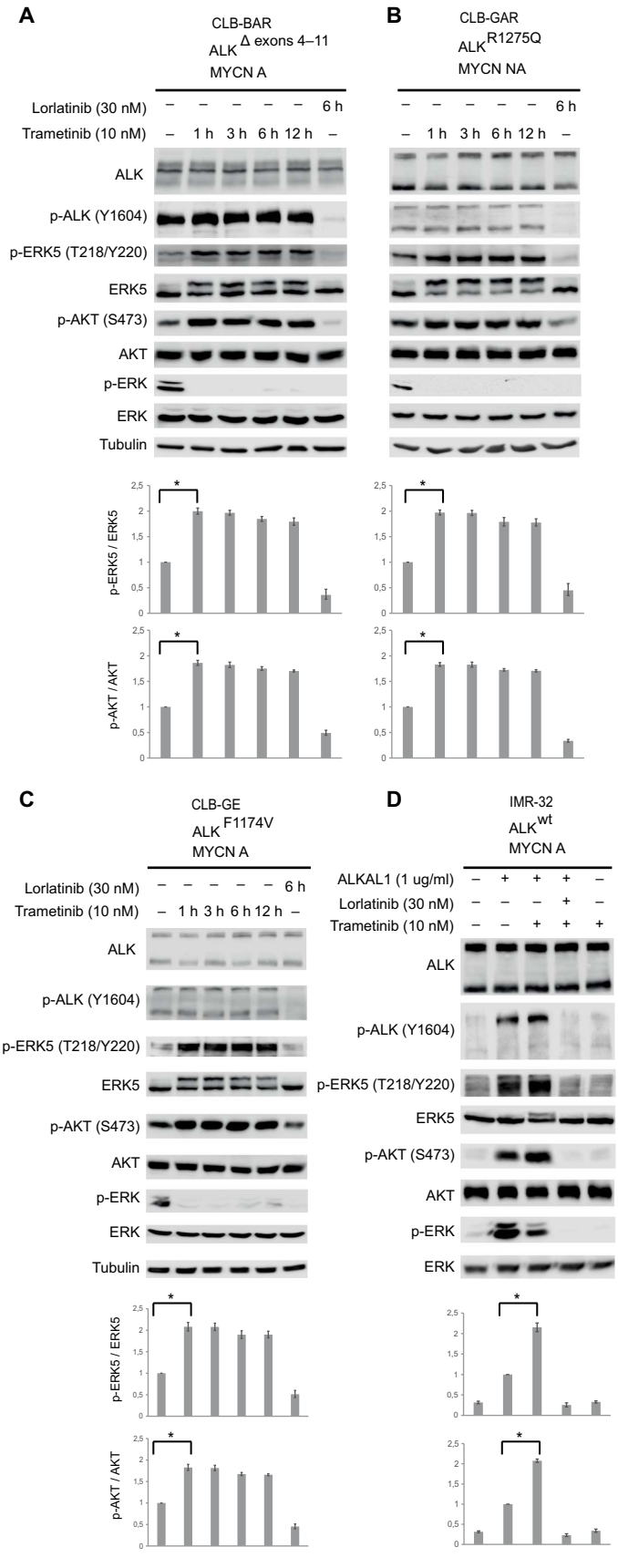

Fig. 2. Specificity of AKT signaling core components in ALK-positive neuroblastoma cell lines. (**A** to **C**) Western blotting for the indicated proteins in lysates from anaplastic lymphoma kinase (ALK)–positive neuroblastoma cell lines CLB-BAR (A), CLB-GAR (B), and CLB-GE (C) treated with trametinib or lorlatinib for the indicated time (h, hours). (**D**) Immunblotting of lysates from IMR32 cells pretreated with trametinib, lorlatinib, or both for 1 hour and then stimulated with ALKAL1 for 30 min. Tubulin (A to C) or total pan–ERK (extracellular signal–regulated kinase) (D) served as loading controls. Data are means ± SE from ≥3 independent experiments. *$P < 0.05$; Student's paired *t* test. wt, wild type.

in ALK-addicted neuroblastoma cells was not observed in EML4-ALK–positive H3122 or DFCI032 cell lines (fig. S5, A and B). These data suggest that, in contrast to the efficacy of trametinib in ALK-positive NSCLC, the increased activation of the AKT signaling core observed in ALK-addicted neuroblastoma cells potentiates ALK signaling output.

mTORC2 drives increased activation of AKT in ALK-addicted neuroblastoma cells

Reactivation of RTK signaling is a plausible mechanism of increased AKT activation after MEK inhibition. However, we performed a phospho-RTK array on lysates from ALK-addicted neuroblastoma cell lines after treatment with trametinib and found no significant reactivation of any RTK (fig. S6A). Another possible mechanism for reactivation of or enhanced signaling to AKT is through the RAS-PI3K-AKT pathway; however, no increase in the abundance of RAS–GTP (guanosine 5′-triphosphate) was detected upon treatment of trametinib, although ERK1/2 phosphorylation was decreased (fig. S6B). Upon RAS-mediated PI3K activation, PI3K phosphorylates phosphatidylinositol 4,5-bisphosphate (PIP2), making phosphatidylinositol 3,4,5-trisphosphate (PIP3) (*44*–*46*). PIP3 recruits proteins, such as AKT, to the membrane through pleckstrin homology domain–mediated binding, leading to activation upon binding to newly formed PIP3. However, similar to the RAS-GTP assay, no increase or decrease in the PIP3/PIP2 lipid ratio was observed upon treatment with trametinib, whereas treatment with lorlatinib (the ALK inhibitor) lowered the PIP3/PIP2 ratio (fig. S6C). These observations suggest that the cross-talk between the MAPK and AKT signaling pathways may be responsible for the increased activation of the AKT signaling core in response to MEK inhibition.

We next determined whether activation of AKT signaling in ALK-addicted neuroblastoma cells in response to trametinib involves the mTOR complexes that have previously been described as master feedback regulators (*47*, *48*) by combining trametinib treatment in ALK-addicted neuroblastoma cell lines (CLB-BAR, CLB-GE, CLB-GAR, and Kelly) with the PI3K inhibitor BEZ235, the mTORC1 and mTORC2 inhibitor AZD8055, or the mTORC1 inhibitor everolimus. As single applications, PI3K and mTORC1/2 inhibition (using BEZ235 and AZD8055, respectively) efficiently blocked the activation of AKT (inferred by phosphorylation at Ser^{473}), but blocking mTORC1 using everolimus increased AKT activation similar to that seen with trametinib (Fig. 3A and fig. S3, A and B). Trametinib alone blocked the phosphorylation (activation) of ERK but not of p70S6K, whereas BEZ235, AZD8055, and everolimus blocked p70S6K but not the activation of ERK (Fig. 3A and fig. S3, A and B). Treatment with everolimus increased the activation of AKT, indicating a role for mTORC1 in this feedback loop (Fig. 3A and fig. S3, A and B). Together, trametinib and everolimus appeared to have an additive effect on the activation status of AKT (Fig. 3A and fig. S3, A and B). Further, increased activation of AKT

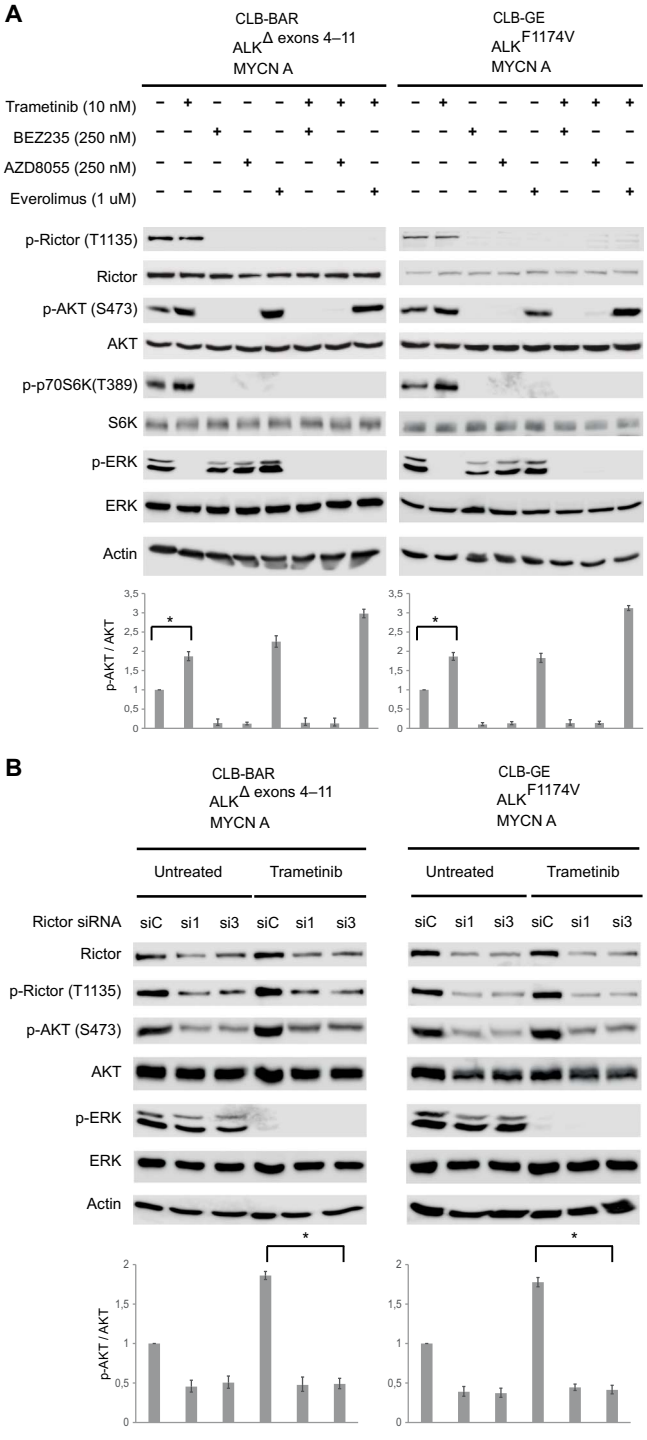

Fig. 3. Trametinib treatment activates AKT signaling via mTORC2. (**A**) ALK-positive neuroblastoma cell lines CLB-BAR and CLB-GE were treated with trametinib, BEZ235, AZD8055, or everolimus either alone or in combination, as indicated. Cell lysates were immunoblotted for p-Rictor (Thr^{1135}), Rictor, p-p70S6K, S6K, p-AKT (Ser^{473}), AKT, p-ERK1/2, and ERK1/2 antibodies. Actin was used as a loading control. (**B**) CLB-BAR and CLB-GE cells were transfected with either scrambled control or two independent siRNAs targeting Rictor before treatment with trametinib. Lysates were separated by SDS–polyacrylamide gel electrophoresis (PAGE) and analyzed for Rictor, p-Rictor (Thr^{1135}), p-Akt (Ser^{473}), AKT, p-ERK1/2, and ERK1/2 abundance by immunoblotting with actin as a loading control. Data are means ± SE from at least three independent experiments. *$P < 0.05$; Student's paired t test.

(phosphorylation at Ser^{473}) after MEK inhibition was independent of the phosphorylation of mTORC2 complex protein Rictor (at Thr^{1135}) (Fig. 3A and fig. S3, A and B). Furthermore, PI3K or mTORC1/2 inhibitors abrogated trametinib-induced activation of AKT, whereas the mTORC1-selective inhibitor everolimus did not (Fig. 3A and fig. S3, A and B), suggesting a role for mTORC2 in the increased activation of AKT signaling in ALK-addicted neuroblastoma cell lines. Assays with the structurally dissimilar mTOR kinase inhibitors rapamycin (an mTORC1 inhibitor) and KU-0063794 (an mTORC1/2 inhibitor) further supported a role for mTORC2 (fig. S7).

To confirm the involvement of the mTORC2 complex in the increased activation of AKT signaling core in ALK-addicted neuroblastoma cell lines upon treatment with trametinib, we inhibited mTORC2 activation using small interfering RNA (siRNA) targeting the mRNA encoding Rictor (Fig. 3B). Compared with cells transfected with control siRNA, cells transfected with one of two independent Rictor siRNAs decreased the basal activation of AKT (Fig. 3B). In response to trametinib, AKT activation increased in control but not in Rictor siRNA–transfected ALK-positive neuroblastoma cells (Fig. 3B). Together, these results suggest a critical role for mTORC2 proteins in MEK inhibitor–induced activation of AKT signaling.

Blocking MEK-ERK signaling enhances AKT activation through SIN1 phosphorylation

Thus far, our data suggest that the RAS-MEK-ERK pathway inhibition in ALK-addicted neuroblastoma cells lead to increased activation of AKT signaling via mTORC2 in a manner that is dependent on the presence of Rictor but independent of its phosphorylation at Thr^{1135}. However, residue Thr^{1135} is important for mTORC2 signaling (*49*); thus, we explored additional components of the mTORC2 complex. The mTORC2 complex includes Rictor, SIN1, and lethal with SEC13 protein 8 (LST8). We started with SIN1, a key regulator of mTORC2 (*50*, *51*). Immunoblotting for phosphorylated SIN1 (at Thr^{86}) in ALK-addicted neuroblastoma cell lines CLB-BAR and CLB-GE revealed that MEK or ERK1/2 inhibition (with trametinib or SCH772984, respectively) increased phosphorylation of SIN1 but that PI3K inhibition (with BEZ235) alone or in combination with either the MEK or ERK1/2 inhibitor reduced SIN1 phosphorylation (Fig. 4A). These observations, together with the results from treatment with AZD8055 inhibitor (Fig. 3A), suggest that RAS-MEK-ERK inhibitor–induced activation of AKT in ALK-addicted neuroblastoma cells occurs through the phosphorylation of SIN1. Knockdown of SIN1 expression using RNA interference inhibited trametinib (MEK inhibitor)–induced AKT activation in ALK-addicted neuroblastoma cells, further supporting the involvement of SIN1 (Fig. 4B). Together, our results indicate that RAS-MEK-ERK pathway inhibition leads to an increased activation of AKT signaling via increased SIN1 Thr^{86} phosphorylation in ALK-addicted neuroblastoma cells.

Treatment with trametinib abrogates tumor growth in ALK-positive NSCLC xenografts but not in ALK-addicted neuroblastoma xenografts

The effect of trametinib was evaluated in BALB/c-nu mice subcutaneously injected with either human neuroblastoma cells (CLB-BAR or SK-N-AS) or EML4-ALK NSCLC cells (H3122). Treatment of mice (by oral gavage) with trametinib inhibited the growth of NSCLC xenografts and that of RAS-mutant SK-N-AS neuroblastoma xenografts (Fig. 5, A and B), similar to the observed inhibition of proliferation in our in vitro assays above and as in previously reported

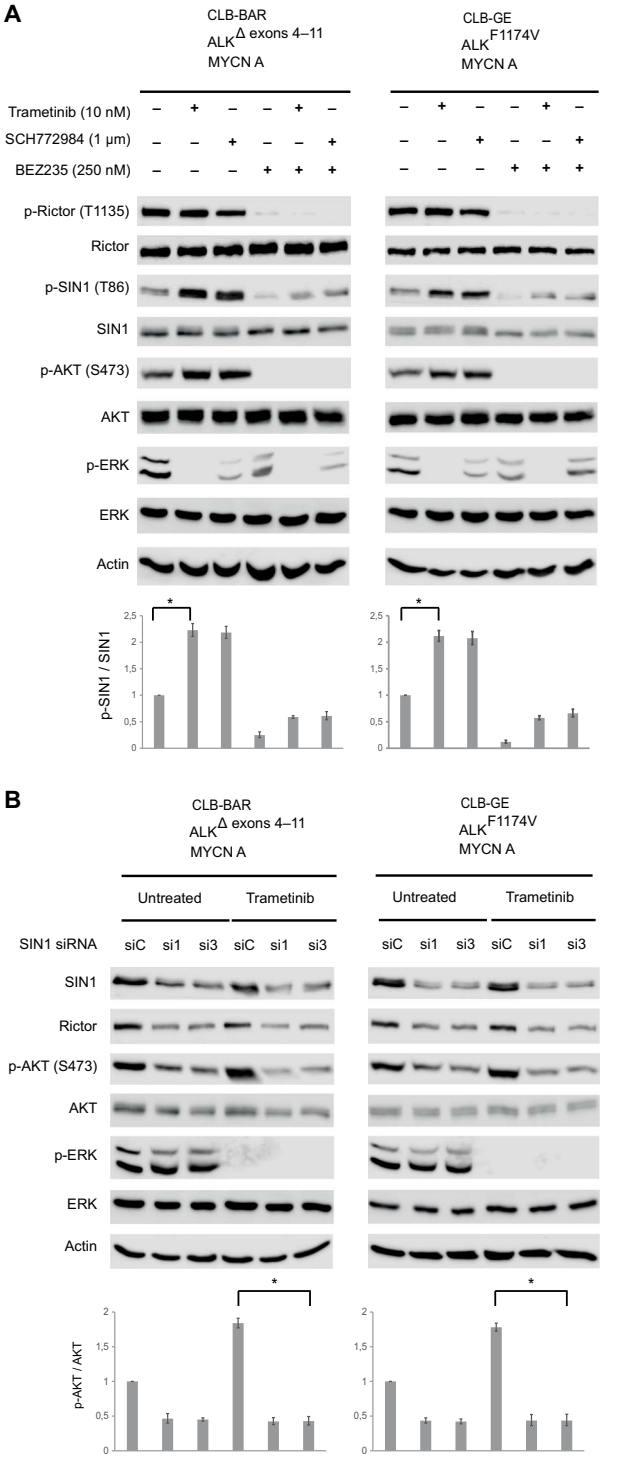

Fig. 4. Knockdown of SIN1 suppresses increased activation of AKT after MEK inhibition. (**A**) Immunoblotting in whole-cell lysates from neuroblastoma cell lines CLB-BAR and CLB-GE grown in complete growth medium and treated with trametinib, SCH772984, BEZ235, or a combination thereof, as indicated. (**B**) Immunoblotting in whole-cell lysates from CLB-BAR and CLB-GE cells treated with trametinib for 1 hour after transfection with scrambled control (siC) or one of two *SIN1*-targeted siRNAs (si1 and si3). Lysates were separated by SDS-PAGE and analyzed for Rictor, SIN1, p-AKT (Ser^{473}), AKT, p-ERK1/2, and ERK1/2 expression by immunoblotting with actin as a loading control. Data are means ± SE from at least three independent experiments. *$P < 0.05$; Student's paired *t* test.

xenografts (*9*, *11*). In contrast, tumor growth inhibition of ALK-addicted CLB-BAR neuroblastoma xenografts was not observed on trametinib treatment when compared to vehicle-treated mice (Fig. 5C). Further, immunoblotting revealed increased AKT phosphorylation in CLB-BAR xenografts excised from mice treated with trametinib, although a decreased phosphorylation of ERK1/2 was observed (fig. S8A), in line with our findings in the cultured cells (Figs. 2 and 3). No sign of distress in the mice was observed upon treatment with trametinib, and the mean body weights in the vehicle- and drug-treated mice were not significantly different (fig. S8B). Thus, although treatment with trametinib is beneficial in tumors harboring ALK fusion protein–driven NSCLC and RAS-mutant neuroblastoma xenografts, it exhibits no beneficial effect on ALK-addicted neuroblastoma xenografts.

DISCUSSION

Whereas monotherapy for cancers with ALK fusions shows promising results, the response of ALK-positive neuroblastoma patients to ALK TKIs as a monotherapy is less encouraging, as reported for crizotinib (*5*, *52*). Lately, new suggestions have appeared from the neuroblastoma field with support from studies using EML4-ALK NSCLC cells that combined inhibition of ALK and the MEK-ERK pathway may be beneficial as a polytherapy in neuroblastoma patients (*8*, *9*, *11*, *53*, *54*). However, our results with various neuroblastoma cell lines suggest that the use of MEK inhibitors is not effective as a single or a polytherapeutic strategy in ALK-positive neuroblastoma.

RTKs signal to both the PI3K and the MAPK pathway, and crosstalk between these two pathways is common, in which inhibition of either pathway can lead to activation of other pathways (*55*–*57*). One possible mechanism upon inhibition of MAPK proteins could be an increased activity of PI3K via Ras-GTP; however, in our hands, no increased PI3K activity was observed (*44*–*46*). Further, a number of feedback mechanisms have been proposed, such as the RAF paradox in melanoma (*6*, *58*–*62*) and involvement of RTKs in the feedback activation mechanisms (*62*, *63*). Other studies have indicated the importance of mTOR kinases and their enigmatic complex activation (*30*, *61*, *64*–*67*). There are two different mTOR complexes, mTORC1 and mTORC2, that respond to different cues, such as growth factors and nutrient availability. Dysregulation of mTOR complexes has been observed in many diseases, such as cancer, obesity, and diabetes (*66*). The mTORC2 complex consists of mTOR subunit, Rictor, SIN1, mLST8, and Protor, and its complex regulation is unresolved. Recently,it was shown that the mTORC2 subunit SIN1 is an AKT substrate in 3T3-L1 adipocytes and human embryonic kidney (HEK) 293 cells, which positively regulates mTORC2 activity (*68*). It has also been reported that, in HeLa cells, S6K is responsible for the phosphorylation of SIN1 in a negative feedback loop between mTORC1 and mTORC2 that inhibits mTORC2 activity (*51*). Studies have indicated that phosphorylation of SIN1 at T86 increases the kinase activity of mTORC2, leading to the phosphorylation of AKT on the S473 site (*67*). We observed that the inhibition of the RAS-MAPK pathway resulted in an increased activation of AKT in ALK-addicted neuroblastoma cell lines, likely occurring through the mTORC2 complex, and identified the SIN1 Thr^{86} phosphorylation of mTORC2 as an important molecular event. Further, reduction of SIN1 expression decreases phosphorylation of AKT on residue 473.

Previous studies have reported that increased AKT phosphorylation after mTORC1 inhibition is dependent on the phosphorylation of Rictor at Thr^{1135} (*65*, *69*), which agrees with our results here. We

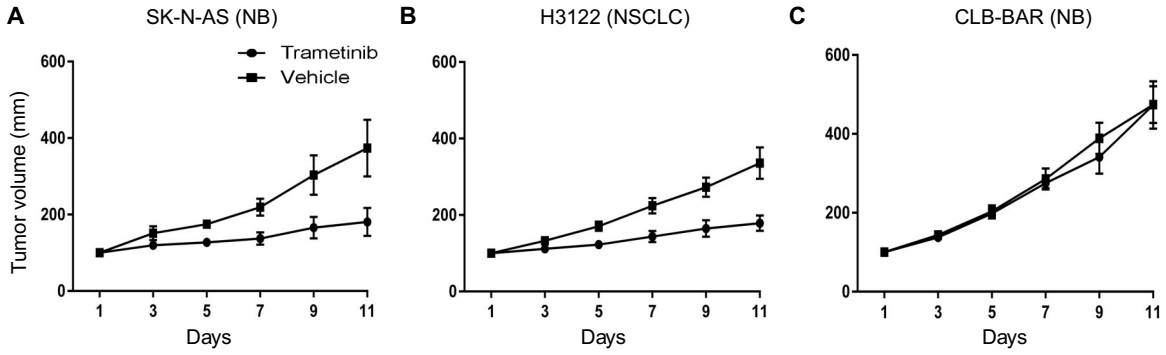

Fig. 5. Efficacy of trametinib in ALK-positive neuroblastoma and NSCLC xenograft models. (**A** to **C**) Growth curves of RAS-positive SK-N-AS neuroblastoma (A; $P \leq 0.05$), EML4-ALK–positive H3122 non–small cell lung cancer (NSCLC) (B; $P \leq 0.05$), or ALK-dependent CLB-BAR neuroblastoma (C; not significantly different by Student's paired *t* test) xenografts in vehicle- and trametinib-treated mice. Data are means ± SD from $n = 6$ mice in each group.

also found that Rictor was required as a partner in the mTORC2 complex but that the phosphorylation of Rictor at Thr^{1135} was not necessary for the increased phosphorylation of AKT after MEK inhibition. A similar increase in AKT phosphorylation was reportedly observed after MEK inhibition in *HER2*-amplified and *EGFR*-mutant cancer cells as a result of ErbB receptor family signaling (*62*). Another report found that long-term treatment of breast cancer cells with inhibitors that block both mTORC1 and mTORC2 induced the activation of PI3K-AKT signaling and increased the protein abundance of EFGR, HER2, HER3, and IRS1 (*63*). A challenging but critical task toward optimizing therapeutic strategies is to understand these complex molecular mechanisms in an individual tumor.

Our results in neuroblastoma cells are in contrast to the behavior of EML4-ALK fusion protein–addicted NSCLC lines that are sensitive to MEK and ERK1/2 inhibitors and do not mediate an increased activation of the AKT protein, consistent with previous reports (*9*). The reason behind this phenomenon is unclear; however, the oncogenic activity of the fusion proteins, such as EML4-ALK, is still dependent on oligomerization and activation driven by the EML4 fusion partner. In contrast, the full-length ALK receptor is located in membranes, it can be further activated by ligands, such as in the IMR32 cell line, although tested cell lines here harbor a receptor with ligand-independent ALK activity. Further, abrogating PI3K or ERK5 signaling does not increase the activation of MAPK pathway in ALK-addicted cell lines (fig. S4A). Abrogation of both ALK and PI3K or ERK5 activity synergistically reduces neuroblastoma cell proliferation and tumor growth (*32*, *33*). It has been suggested that increased AKT signaling could attenuate anticancer efficacy, confer resistance, and/or contribute to the development of resistance (*47*, *48*). Further, reducing mTORC2 activity decreases HIF2α mRNA and protein expression correlating with smaller and less vascularized tumors from metastatic tumor xenografts (*70*).

Future investigation will be needed to clarify whether MEK or ERK1/2 is responsible directly or indirectly for the phosphorylation of Thr^{86} of SIN1 at the molecular level. Alternatively, they may negatively regulate a SIN1 phosphatase mediating the cross-talk mechanisms between the RAS-MAPK pathway and mTORC2. An additional hypothesis is that MEK-ERK mediates a negative feedback loop on SIN1 because the phosphorylation status of RICTOR, an mTORC2 complex member, at residue 1135 does not appear to be important in ALK-positive neuroblastoma and has been reported to not affect mTORC2 kinase activity (*49*, *69*, *71*, *72*).

This study revealed that treatment of ALK-addicted neuroblastoma cells or xenografts with MEK/ERK inhibitor does not abrogate cell or tumor growth. Our data are supported by reports indicating that other ALK-addicted cell lines do not respond to binimetinib, an orally bioavailable inhibitor of MEK1/2 (IC_{50} = 12 nM) as a single agent or in combination with ALK inhibitor, although binimetinib is an effective inhibitor against neuroblastoma tumor cells with activated RAS or low NF1 expression (*12*, *13*, *73*). Our results highlight a mechanism upon MEK/ERK inhibition in an ALK-addicted neuroblastoma background because treatment results in an increased activation of AKT-ERK5 signaling under these circumstances. These results indicate that a combination of ALK inhibitors with MEK/ERK inhibitors is not motivated as a treatment option for ALK-addicted neuroblastoma in the clinic, reflecting the need to fully understand the complex molecular mechanisms involved before considering combinatorial treatment in neuroblastoma patients.

MATERIALS AND METHODS

High-resolution SNP array

DNA from nine cell lines was analyzed for copy number changes using CytoScan HD (Affymetrix Inc.). The CytoScan HD, with about 2.7×10^6 milk probes, has a mean marker distance of one marker per 1 kilobase pair. The cell lines were CLB-BAR, CLB-GE, CLB-GAR, Kelly, SK-N-DZ, CLB-PE, IMR32, SK-N-AS, and SK-N-BE. All CLB lines are from Centre Léon Bérard under a material transfer agreement (MTA). The array experiments were performed according to the protocol provided by the supplier. Briefly, total genomic DNA (250 ng) was digested with the restriction enzyme and ligated to adaptors. After ligation, the template was subjected to polymerase chain reaction (PCR) amplification using a generic primer that recognizes the adaptor sequence. The purified PCR products were fragmented with deoxyribonuclease I, labeled with biotin, and hybridized to a GeneChip Human Mapping array. The hybridized probes were washed using the Affymetrix Fluidics Station 450 and marked with streptavidin-phycoerythrin. The arrays were scanned using a confocal laser scanner, GeneChip Scanner 3000 (Affymetrix). GeneChip Operating Software and GeneChip Genotyping Analysis Software (Affymetrix) were used for primary data analysis, normalization against internal control features on the chip, genotype calling, and quality control. Subsequent analysis was then performed using copy number analyzer for GeneChip (CNAG 3.5.1, Genome Laboratory, Tokyo University) (www.genome.umin.jp) featuring the algorithm for allele-specific copy number analysis using AsCNAR (anonymous references). In CNAG, the tumor samples were compared in silico to the eight best-matched control samples (lowest SD)

available among a set of nonmatched healthy individuals. This set contained both HapMap samples available from Affymetrix and our own set of healthy control samples. We also used Chromosome Analysis Suite software (ChAS v. 2.0.0.195, Affymetrix) to perform the cytogenetics analysis. All cases of chromosomal gain, loss, or amplification were scored for both segmental and numerical aberrations, including detailed information about the breakpoint positions when applicable. Chromosomal positions (in table S1) are given according to human genome build GRCh37/hg19. Determination of genomic profile (Table 1) was carried out essentially in the same way we have done previously (*74*).

DNA sequencing of *ALK*, *TP53*, and *NRAS* regions according to Sanger

Sanger sequencing was performed for DNAs from the nine cell lines. The sequenced regions were exons 21 to 26 for ALK (cover amino acid positions 1120 to 1313), exons 5 to 10 for TP53 (cover amino acid positions 33 to 367), and exons 2 and 3 for NRAS (cover amino acid positions 1 to 97). Touchdown PCR was performed in 10-μl reactions using AmpliTaq Gold DNA Polymerase (Thermo Fisher Scientific), forward and reverse primers (10 μM each), and 20 ng of cell line DNA. The PCR program was performed as follows: 95°C for 5 min, before 20 cycles of 95°C for 30 s, 65°C for 30 s (decreasing by 0.5°C in every cycle), and 72°C for 1 min, followed by 16 cycles of 95°C for 30 s, 55°C for 30 s, and 72°C for 1 min, and ending with an extension step at 72°C for 7 min. The specificity of products was inspected by agarose gel electrophoresis before they were purified using Agencourt AMPure magnetic beads (Beckman Coulter) using the Biomek NX pipetting robot (Beckman Coulter) and eluted in distilled H_2O. Sequence PCR was performed using the BDT (BigDye Terminator) v3.1 Cycle Sequencing kit (Applied Biosystems) in 10-μl reactions containing 6 μl of 1:3 diluted PCR/template DNA and 1 μl each of BDT, 1× BDT buffer, and 1.6 μM forward and reverse PCR primers. Sequence PCR was run under the following conditions: 94°C for 3 min, followed by 50 cycles of 96°C for 30 s, 50°C for 10 s, and 60°C for 3 min each. Sequencing products were purified using CleanSeq magnetic beads (Agencourt) using the Biomek NX and resuspended in Hi-Di formamide (10 μl; Applied Biosystems). Sequencing products were separated with gel electrophoresis on a 3730 DNA analyzer (Applied Biosystems), and the output data were viewed and analyzed using SeqScape v2.5 (Applied Biosystems). All of the fragments were analyzed with both forward and reverse primers, and all of the findings were confirmed by sequencing of a new PCR product. Sequencing was performed in-house or at GATC Biotech AG, European Custom Sequencing Center (Germany).

Antibodies, cell lines, and reagents

Pan-ERK1/2 antibody (1:5000; cat. #610123) was purchased from BD Transduction Laboratories. Phospho-ALK (1:1000; Y1604; #3341), phospo-ERK5 (1:1000; T218/Y220; cat. #3371), ERK5 (1:2000; cat. #3372), phospho-AKT (1:5000; Ser473; #4060), AKT (1:10000; cat. #9272), Rictor (1:1000; #2114), phospho-Rictor (1:1000; T1135; #3806), SIN1 (1:000; #12860), phospho-SIN1 (1:1000; T86; #14716), phospho-p70 S6 kinase (1:1000; Thr389; #9234), S6K (1:2000; cat. #9202), p44/42 MAPK (1:5000; ERK1/2; #9102), β-actin (1:10000; #4970), and tubulin (1:10000; #2144) antibodies were from Cell Signaling Technology. Horseradish peroxidase (HRP)–conjugated secondary antibody, goat anti-mouse immunoglobulin G (IgG), and goat anti-rabbit IgG (1:5000) were purchased from Thermo Fisher Scientific. ALKAL (FAM150A) was used as described previously (*41*). Trametinib, SCH772984, BEZ235, AZD8055, XMD8-92, and everolimus (RAD001) were from Selleckchem. The H3122 and DFCI032 cell lines were gifts from R. George and P. Jänne (Dana-Farber Cancer Institute). All neuroblastoma and NSCLC cell lines were cultured in RPMI 1640 or Dulbecco's modified Eagle's medium with 10% fetal bovine serum and 1% penicillin and streptomycin.

Immunoblotting

Cells were lysed on ice with hypotonic lysis buffer [20 mM tris-HCl (pH 7.5), 150 mM NaCl, 1 mM EDTA, 1 mM EGTA, 1% Triton, 2.5 mM sodium pyrophosphate, 1 mM β-glycerophosphate, 1 mM Na_3VO_4, and leupeptin (1 μg/ml), with protease/phosphatase inhibitor cocktail (Cell Signaling Technology)] for 15 min and then centrifuged for 10 min at 4°C. The proteins were separated on 7.5% bis-acryl-tris gels, transferred to polyvinylidene difluoride membranes (Millipore), blocked in 5% bovine serum albumin (phosphoprotein blots) or 5% milk, and immunoblotted against primary antibodies overnight at 4°C. Secondary antibodies were diluted 1:10,000 and incubated with shaking at room temperature for 1 hour. Enhanced chemiluminescence substrates were used for detection (GE Healthcare). Antibody dilutions are noted in the section above.

Viability assay

Cell viability was assessed as relative redox metabolic activity using a resazurin-based assay. CLB-BAR, CLB-GE, CLB-GA, Kelly, SK-N-AS, SK-N-BE, SK-N-DZ, IMR32, and CLB-PE neuroblastoma cells (0.2×10^5) were plated on collagen-coated 24-well plates. Cells were treated with inhibitors, as indicated in the figures, and monitored for 12 days, refreshing the medium and inhibitor dose every third day. Cells were incubated with 55 μM resazurin (Sigma-Aldrich) for 3 hours at 37°C. Metabolized resazurin was analyzed by plate reader (TEKAN) as relative fluorescence. For combination treatments, 0.4×10^5 cells were plated on collagen-coated 48-well plates, treated as indicated in the figures, and monitored for 5 days. Cell viability was assessed as described for single-inhibitor assays.

SiRNA transfection

CLB-BAR and CLB-GE cell lines were transfected with one of two duplex siRNAs targeting *RICTOR* and *SIN1* (Stealth RNAi, Invitrogen) according to the manufacturer's protocols. Cells transfected with scrambled siRNA (Invitrogen) were used as negative controls.

Phospho-RTK array

ALK-positive neuroblastoma cell line lysates (400 μg) were incubated on human phospho-RTK membrane array according to the manufacturer's instruction (ARY001B, R&D Systems). Phospho-RTK abundances were assessed using HRP-conjugated pan-phosphotyrosine antibody, followed by chemiluminescence detection.

PIP mass quantification

Phospholipids were isolated from CLB-BAR neuroblastoma cells, and PIP abundance was measured using an enzyme-linked immunosorbent assay kit (Echelon Biosciences) according to the manufacturer's protocol.

Active Ras assay

For detecting active Ras, cells were plated on a 10-cm plate and treated with trametinib for 3 hours. Active Ras was measured using Active Ras

Detection kit (Cell Signaling Technology) according to the manufacturer's protocol.

Subcutaneous xenografts

Female BALB/cAnNRj-Foxn1nu mice (Janvier Laboratory) at 5 to 6 weeks of age were subcutaneously injected with 2.5×10^6 CLB-BAR, H3122, or SK-N-AS cells in serum-free medium mixed at a ratio of 1:1 with Matrigel Matrix (lot. #6140322, Corning), at a total injection volume of 100 µl, into the left flank. Once tumor volume reached an average of 100 to 150 mm^3, the mice were randomized to treatment groups. Drug was given daily at 3 mg/kg body weight by oral gavage, continuously for 12 days. Tumor volume was measured by calipers every other day and calculated by the following equation: $V = (\pi/6) \times L \times W^2$ (V, volume; L, length; W, width). The vehicle for trametenib was 10% Kollisolv PEG E 400 (06855, lot. #BCBQ6662V, Sigma-Aldrich) and 10% Kolliphor EL (C5135, lot. #BCBQ5632V, Sigma-Aldrich).

Statistical analysis

Statistical analyses of the data were performed by Student's paired t test. All quantitative analysis were presented as means ± SD, as indicated. Measurements were log-transformed to meet normality assumption before analyses. $P < 0.05$ was considered significant.

SUPPLEMENTARY MATERIALS

www.sciencesignaling.org/cgi/content/full/10/507/eaam7550/DC1
Fig. S1. SNP array genome profiles of the nine neuroblastoma cell lines.
Fig. S2. NF1 abundance in neuroblastoma cell lines.
Fig. S3. Sensitivity of neuroblastoma cell lines to trametinib.
Fig. S4. AKT signaling inhibition does not lead to increased activation of MAPK.
Fig. S5. Sensitivity of EML4-ALK–positive NSCLC cell lines to trametinib.
Fig. S6. Phospho-RTK array analysis after MEK inhibition.
Fig. S7. Increased AKT activation in cells upon treatment with trametinib and rapamycin.
Fig. S8. Increased AKT activation in xenografts upon treatment with trametinib.
Table S1. Chromosomal profiles of the cell lines.
Table S2. Trametinib does not act synergistically with lorlatinib to inhibit ALK-positive neuroblastoma cell line proliferation.
Reference (*76*)

REFERENCES AND NOTES

1. D. Fey, D. Matallanas, J. Rauch, O. S. Rukhlenko, B. N. Kholodenko, The complexities and versatility of the RAS-to-ERK signalling system in normal and cancer cells. *Semin. Cell Dev. Biol.* **58**, 96–107 (2016).
2. H. Abe, S. Kikuchi, K. Hayakawa, T. Iida, N. Nagahashi, K. Maeda, J. Sakamoto, N. Matsumoto, T. Miura, K. Matsumura, N. Seki, T. Inaba, H. Kawasaki, T. Yamaguchi, R. Kakefuda, T. Nanayama, H. Kurachi, Y. Hori, T. Yoshida, J. Kakegawa, Y. Watanabe, A. G. Gilmartin, M. C. Richter, K. G. Moss, S. G. Laquerre, Discovery of a highly potent and selective MEK inhibitor: GSK1120212 (JTP-74057 DMSO solvate). *ACS Med. Chem. Lett.* **2**, 320–324 (2011).
3. A. G. Gilmartin, M. R. Bleam, A. Groy, K. G. Moss, E. A. Minthorn, S. G. Kulkarni, C. M. Rominger, S. Erskine, K. E. Fisher, J. Yang, F. Zappacosta, R. Annan, D. Sutton, S. G. Laquerre, GSK1120212 (JTP-74057) is an inhibitor of MEK activity and activation with favorable pharmacokinetic properties for sustained in vivo pathway inhibition. *Clin. Cancer Res.* **17**, 989–1000 (2011).
4. T. Yamaguchi, R. Kakefuda, N. Tajima, Y. Sowa, T. Sakai, Antitumor activities of JTP-74057 (GSK1120212), a novel MEK1/2 inhibitor, on colorectal cancer cell lines in vitro and in vivo. *Int. J. Oncol.* **39**, 23–31 (2011).
5. Y. P. Mossé, M. S. Lim, S. D. Voss, K. Wilner, K. Ruffner, J. Laliberte, D. Rolland, F. M. Balis, J. M. Maris, B. J. Weigel, A. M. Ingle, C. Ahern, P. C. Adamson, S. M. Blaney, Safety and activity of crizotinib for paediatric patients with refractory solid tumours or anaplastic large-cell lymphoma: A Children's Oncology Group phase 1 consortium study. *Lancet Oncol.* **14**, 472–480 (2013).
6. E. M. Tricker, C. Xu, S. Uddin, M. Capelletti, D. Ercan, A. Ogino, C. A. Pratilas, N. Rosen, N. S. Gray, K.-K. Wong, P. A. Jänne, Combined EGFR/MEK inhibition prevents the emergence of resistance in *EGFR*-mutant lung cancer. *Cancer Discov.* **5**, 960–971 (2015).
7. K. R. Bosse, J. M. Maris, Advances in the translational genomics of neuroblastoma: From improving risk stratification and revealing novel biology to identifying actionable genomic alterations. *Cancer* **122**, 20–33 (2016).
8. T. F. Eleveld, D. A. Oldridge, V. Bernard, J. Koster, L. C. Daage, S. J. Diskin, L. Schild, N. B. Bentahar, A. Bellini, M. Chicard, E. Lapouble, V. Combaret, P. Legoix-Né, J. Michon, T. J. Pugh, L. S. Hart, J. Rader, E. F. Attiyeh, J. S. Wei, S. Zhang, A. Naranjo, J. M. Gastier-Foster, M. D. Hogarty, S. Asgharzadeh, M. A. Smith, J. M. Guidry Auvil, T. B. K. Watkins, D. A. Zwijnenburg, M. E. Ebus, P. van Sluis, A. Hakkert, E. van Wezel, C. E. van der Schoot, E. M. Westerhout, J. H. Schulte, G. A. Tytgat, M. E. M. Dolman, I. Janoueix-Lerosey, D. S. Gerhard, H. N. Caron, O. Delattre, J. Khan, R. Versteeg, G. Schleiermacher, J. J. Molenaar, J. M. Maris, Relapsed neuroblastomas show frequent RAS-MAPK pathway mutations. *Nat. Genet.* **47**, 864–871 (2015).
9. G. Hrustanovic, V. Olivas, E. Pazarentzos, A. Tulpule, S. Asthana, C. M. Blakely, R. A. Okimoto, L. Lin, D. S. Neel, A. Sabnis, J. Flanagan, E. Chan, M. Varella-Garcia, D. L. Aisner, A. Vaishnavi, S.-H. I. Ou, E. A. Collisson, E. Ichihara, P. C. Mack, C. M. Lovly, N. Karachaliou, R. Rosell, J. W. Riess, R. C. Doebele, T. G. Bivona, RAS-MAPK dependence underlies a rational polytherapy strategy in EML4-ALK–positive lung cancer. *Nat. Med.* **21**, 1038–1047 (2015).
10. M. K. Kiessling, A. Curioni-Fontecedro, P. Samaras, S. Lang, M. Scharl, A. Aguzzi, D. A. Oldrige, J. M. Maris, G. Rogler, Targeting the mTOR complex by Everolimus in NRAS mutant neuroblastoma. *PLOS ONE* **11**, e0147682 (2016).
11. E. Manchado, S. Weissmueller, J. P. Morris, C.-C. Chen, R. Wullenkord, A. Lujambio, E. de Stanchina, J. T. Poirier, J. F. Gainor, R. B. Corcoran, J. A. Engelman, C. M. Rudin, N. Rosen, S. W. Lowe, A combinatorial strategy for treating KRAS-mutant lung cancer. *Nature* **534**, 647–651 (2016).
12. S. E. Woodfield, L. Zhang, K. A. Scorsone, Y. Liu, P. E. Zage, Binimetinib inhibits MEK and is effective against neuroblastoma tumor cells with low NF1 expression. *BMC Cancer* **16**, 172 (2016).
13. L. S. Hart, J. Rader, P. Raman, V. Batra, M. R. Russell, M. Tsang, M. Gagliardi, L. Chen, D. Martinez, Y. Li, A. Wood, S. Kim, S. Parasuraman, S. Delach, K. A. Cole, S. Krupa, M. Boehm, M. Peters, G. Caponigro, J. M. Maris, Preclinical therapeutic synergy of MEK1/2 and CDK4/6 inhibition in neuroblastoma. *Clin. Cancer Res.* **23**, 1785–1796 (2017).
14. J. M. Maris, Recent advances in neuroblastoma. *N. Engl. J. Med.* **362**, 2202–2211 (2010).
15. J. M. Maris, M. D. Hogarty, R. Bagatell, S. L. Cohn, Neuroblastoma. *Lancet* **369**, 2106–2120 (2007).
16. K. K. Matthay, J. M. Maris, G. Schleiermacher, A. Nakagawara, C. L. Mackall, L. Diller, W. A. Weiss, Neuroblastoma. *Nat. Rev. Dis. Primers* **2**, 16078 (2016).
17. J. R. Park, R. Bagatell, W. B. London, J. M. Maris, S. L. Cohn, K. M. Mattay, M. Hogarty; COG Neuroblastoma Committee, Children's Oncology Group's 2013 blueprint for research: Neuroblastoma. *Pediatr. Blood Cancer* **60**, 985–993 (2013).
18. S. Goto, S. Umehara, R. B. Gerbing, D. O. Stram, G. M. Brodeur, R. C. Seeger, J. N. Lukens, K. K. Matthay, H. Shimada, Histopathology (International Neuroblastoma Pathology Classification) and MYCN status in patients with peripheral neuroblastic tumors: A report from the Children's Cancer Group. *Cancer* **92**, 2699–2708 (2001).
19. S. De Brouwer, K. De Preter, C. Kumps, P. Zabrocki, M. Porcu, E. M. Westerhout, A. Lakeman, J. Vandesompele, J. Hoebeeck, T. Van Maerken, A. De Paepe, G. Laureys, J. H. Schulte, A. Schramm, C. Van Den Broecke, J. Vermeulen, N. Van Roy, K. Beiske, M. Renard, R. Noguera, O. Delattre, I. Janoueix-Lerosey, P. Kogner, T. Martinsson, A. Nakagawara, M. Ohira, H. Caron, A. Eggert, J. Cools, R. Versteeg, F. Speleman, Meta-analysis of neuroblastomas reveals a skewed *ALK* mutation spectrum in tumors with *MYCN* amplification. *Clin. Cancer Res.* **16**, 4353–4362 (2010).
20. T. J. Pugh, O. Morozova, E. F. Attiyeh, S. Asgharzadeh, J. S. Wei, D. Auclair, S. L. Carter, K. Cibulskis, M. Hanna, A. Kiezun, J. Kim, M. S. Lawrence, L. Lichenstein, A. McKenna, C. Sekhar Pedamallu, A. H. Ramos, E. Shefler, A. Sivachenko, C. Sougnez, C. Stewart, A. Ally, I. Birol, R. Chiu, R. D. Corbett, M. Hirst, S. D. Jackman, B. Kamoh, A. Hadj Khodabakshi, M. Krzywinski, A. Lo, R. A. Moore, K. L. Mungall, J. Qian, A. Tam, N. Thiessen, Y. Zhao, K. A. Cole, M. Diamond, S. J. Diskin, Y. P. Mosse, A. C. Wood, L. Ji, R. Sposto, T. Badgett, W. B. London, Y. Moyer, J. M. Gastier-Foster, M. A. Smith, J. M. Guidry Auvil, D. S. Gerhard, M. D. Hogarty, S. J. M. Jones, E. S. Lander, S. B. Gabriel, G. Getz, R. C. Seeger, J. Khan, M. A. Marra, M. Meyerson, J. M. Maris, The genetic landscape of high-risk neuroblastoma. *Nat. Genet.* **45**, 279–284 (2013).
21. H. Caren, F. Abel, P. Kogner, T. Martinsson, High incidence of DNA mutations and gene amplifications of the ALK gene in advanced sporadic neuroblastoma tumours. *Biochem. J.* **416**, 153–159 (2008).
22. Y. Chen, J. Takita, Y. Lim Choi, M. Kato, M. Ohira, M. Sanada, L. Wang, M. Soda, A. Kikuchi, T. Igarashi, A. Nakagawara, Y. Hayashi, H. Mano, S. Ogawa, Oncogenic mutations of ALK kinase in neuroblastoma. *Nature* **455**, 971–974 (2008).
23. R. E. George, T. Sanda, M. Hanna, S. Fröhling, W. Luther II, J. Zhang, Y. Ahn, W. Zhou, W. B. London, P. McGrady, L. Xue, S. Zozulya, V. E. Gregor, T. R. Webb, N. S. Gray, D. Gary Gilliland, L. Diller, H. Greulich, S. W. Morris, M. Meyerson, A. T. Look, Activating mutations in ALK provide a therapeutic target in neuroblastoma. *Nature* **455**, 975–978 (2008).

24. I. Janoueix-Lerosey, D. Lequin, L. Brugières, A. Ribeiro, L. de Pontual, V. Combaret, V. Raynal, A. Puisieux, G. Schleiermacher, G. Pierron, D. Valteau-Couanet, T. Frebourg, J. Michon, S. Lyonnet, J. Amiel, O. Delattre, Somatic and germline activating mutations of the ALK kinase receptor in neuroblastoma. *Nature* **455**, 967–970 (2008).
25. Y. P. Mossé, M. Laudenslager, L. Longo, K. A. Cole, A. Wood, E. F. Attiyeh, M. J. Laquaglia, R. Sennett, J. E. Lynch, P. Perri, G. Laureys, F. Speleman, C. Kim, C. Hou, H. Hakonarson, A. Torkamani, N. J. Schork, G. M. Brodeur, G. P. Tonini, E. Rappaport, M. Devoto, J. M. Maris, Identification of *ALK* as a major familial neuroblastoma predisposition gene. *Nature* **455**, 930–935 (2008).
26. A. Bellini, V. Bernard, Q. Leroy, T. R. Frio, G. Pierron, V. Combaret, E. Lapouble, N. Clement, H. Rubie, E. Thebaud, P. Chastagner, A. S. Defachelles, C. Bergeron, N. Buchbinder, S. Taque, A. Auvrignon, D. Valteau-Couanet, J. Michon, I. Janoueix-Lerosey, O. Delattre, G. Schleiermacher, Deep sequencing reveals occurrence of subclonal ALK mutations in neuroblastoma at diagnosis. *Clin. Cancer Res.* **21**, 4913–4921 (2015).
27. T. Martinsson, T. Eriksson, J. Abrahamsson, H. Caren, M. Hansson, P. Kogner, S. Kamaraj, C. Schönherr, J. Weinmar, K. Ruuth, R. H. Palmer, B. Hallberg, Appearance of the novel activating F1174S ALK mutation in neuroblastoma correlates with aggressive tumor progression and unresponsiveness to therapy. *Cancer Res.* **71**, 98–105 (2011).
28. G. Schleiermacher, N. Javanmardi, V. Bernard, Q. Leroy, J. Cappo, T. R. Frio, G. Pierron, E. Lapouble, V. Combaret, F. Speleman, B. de Wilde, A. Djos, I. Øra, F. Hedborg, C. Träger, B.-M. Holmqvist, J. Abrahamsson, M. Peuchmaur, J. Michon, I. Janoueix-Lerosey, P. Kogner, O. Delattre, T. Martinsson, Emergence of new *ALK* mutations at relapse of neuroblastoma. *J. Clin. Oncol.* **32**, 2727–2734 (2014).
29. Z. Chen, T. Sasaki, X. Tan, J. Carretero, T. Shimamura, D. Li, C. Xu, Y. Wang, G. O. Adelmant, M. Capelletti, H. J. Lee, S. J. Rodig, C. Borgman, S.-i. Park, H. R. Kim, R. Padera, J. A. Marto, N. S. Gray, A. L. Kung, G. I. Shapiro, P. A. Jänne, K.-K. Wong, Inhibition of ALK, PI3K/MEK, and HSP90 in murine lung adenocarcinoma induced by *EML4*-ALK fusion oncogene. *Cancer Res.* **70**, 9827–9836 (2010).
30. C. Wang, A. Cigliano, S. Delogu, J. Armbruster, F. Dombrowski, M. Evert, X. Chen, D. F. Calvisi, Functional crosstalk between AKT/mTOR and Ras/MAPK pathways in hepatocarcinogenesis: Implications for the treatment of human liver cancer. *Cell Cycle* **12**, 1999–2010 (2013).
31. Y.-K. Yoon, H.-P. Kim, S.-W. Han, H.-S. Hur, D. Y. Oh, S.-A. Im, Y.-J. Bang, T.-Y. Kim, Combination of EGFR and MEK1/2 inhibitor shows synergistic effects by suppressing EGFR/HER3-dependent AKT activation in human gastric cancer cells. *Mol. Cancer Ther.* **8**, 2526–2536 (2009).
32. N. F. Moore, A. M. Azarova, N. Bhatnagar, K. N. Ross, L. E. Drake, S. Frumm, Q. S. Liu, A. L. Christie, T. Sanda, L. Chesler, A. L. Kung, N. S. Gray, K. Stegmaier, R. E. George, Molecular rationale for the use of PI3K/AKT/mTOR pathway inhibitors in combination with crizotinib in *ALK*-mutated neuroblastoma. *Oncotarget* **5**, 8737–8749 (2014).
33. G. Umapathy, A. El Wakil, B. Witek, L. Chesler, L. Danielson, X. Deng, N. S. Gray, M. Johansson, S. Kvarnbrink, K. Ruuth, C. Schönherr, R. H. Palmer, B. Hallberg, The kinase ALK stimulates the kinase ERK5 to promote the expression of the oncogene MYCN in neuroblastoma. *Sci. Signal.* **7**, ra102 (2014).
34. C. Schönherr, K. Ruuth, Y. Yamazaki, T. Eriksson, J. Christensen, R. H. Palmer, B. Hallberg, Activating ALK mutations found in neuroblastoma are inhibited by Crizotinib and NVP-TAE684. *Biochem. J.* **440**, 405–413 (2011).
35. J. T. Siaw, H. Wan, K. Pfeifer, V. M. Rivera, J. Guan, R. H. Palmer, B. Hallberg, Brigatinib, an anaplastic lymphoma kinase inhibitor, abrogates activity and growth in ALK-positive neuroblastoma cells, *Drosophila* and mice. *Oncotarget* **7**, 29011–29022 (2016).
36. J. Guan, E. R. Tucker, H. Wan, D. Chand, L. S. Danielson, K. Ruuth, A. El Wakil, B. Witek, Y. Jamin, G. Umapathy, S. P. Robinson, T. W. Johnson, T. Smeal, T. Martinsson, L. Chesler, R. H. Palmer, B. Hallberg, The ALK inhibitor PF-06463922 is effective as a single agent in neuroblastoma driven by expression of ALK and MYCN. *Dis. Model. Mech.* **9**, 941–952 (2016).
37. D. Han, B. A. Spengler, R. A. Ross, Increased wild-type N-ras activation by neurofibromin down-regulation increases human neuroblastoma stem cell malignancy. *Genes Cancer* **2**, 1034–1043 (2011).
38. D. W. Coulter, J. Blatt, A. J. D'Ercole, B. M. Moats-Staats, IGF-I receptor inhibition combined with rapamycin or temsirolimus inhibits neuroblastoma cell growth. *Anticancer Res.* **28**, 1509–1516 (2008).
39. C.-K. Shiau, D.-L. Gu, C.-F. Chen, C.-H. Lin, Y.-S. Jou, IGRhCellID: Integrated genomic resources of human cell lines for identification. *Nucleic Acids Res.* **39**, D520–D524 (2011).
40. N. R. Infarinato, J. H. Park, K. Krytska, H. T. Ryles, R. Sano, K. M. Szigety, Y. Li, H. Y. Zou, N. V. Lee, T. Smeal, M. A. Lemmon, Y. P. Mossé, The ALK/ROS1 inhibitor PF-06463922 overcomes primary resistance to crizotinib in ALK-driven neuroblastoma. *Cancer Discov.* **6**, 96–107 (2016).
41. J. Guan, G. Umapathy, Y. Yamazaki, G. Wolfstetter, P. Mendoza, K. Pfeifer, A. Mohammed, F. Hugosson, H. Zhang, A. W. Hsu, R. Halenbeck, B. Hallberg, R. H. Palmer, FAM150A and FAM150B are activating ligands for anaplastic lymphoma kinase. *eLife* **4**, e09811 (2015).
42. A. V. Reshetnyak, P. B. Murray, X. Shi, E. S. Mo, J. Mohanty, F. Tome, H. Bai, M. Gunel, I. Lax, J. Schlessinger, Augmentor α and β (FAM150) are ligands of the receptor tyrosine kinases ALK and LTK: Hierarchy and specificity of ligand-receptor interactions. *Proc. Natl. Acad. Sci. U.S.A.* **112**, 15862–15867 (2015).
43. J. Guan, G. Wolfstetter, J. Siaw, D. Chand, F. Hugosson, R. H. Palmer, B. Hallberg, Anaplastic lymphoma kinase L1198F and G1201E mutations identified in anaplastic thyroid cancer patients are not ligand-independent. *Oncotarget* **8**, 11566–11578 (2017).
44. T. Kodaki, R. Woscholski, B. Hallberg, P. Rodriguez-Viciana, J. Downward, P. J. Parker, The activation of phosphatidylinositol 3-kinase by Ras. *Curr. Biol.* **4**, 798–806 (1994).
45. L. E. Rameh, L. C. Cantley, The role of phosphoinositide 3-kinase lipid products in cell function. *J. Biol. Chem.* **274**, 8347–8350 (1999).
46. P. Rodriguez-Viciana, P. H. Warne, R. Dhand, B. Vanhaesebroeck, I. Gout, M. J. Fry, M. D. Waterfield, J. Downward, Phosphatidylinositol-3-OH kinase as a direct target of Ras. *Nature* **370**, 527–532 (1994).
47. N. Hay, The Akt-mTOR tango and its relevance to cancer. *Cancer Cell* **8**, 179–183 (2005).
48. N. Rosen, Q. B. She, AKT and cancer—Is it all mTOR? *Cancer Cell* **10**, 254–256 (2006).
49. L.-A. Julien, A. Carriere, J. Moreau, P. P. Roux, mTORC1-activated S6K1 phosphorylates Rictor on threonine 1135 and regulates mTORC2 signaling. *Mol. Cell. Biol.* **30**, 908–921 (2010).
50. E. Jacinto, V. Facchinetti, D. Liu, N. Soto, S. Wei, S. Yun Jung, Q. Huang, J. Qin, SIN1/MIP1 maintains rictor-mTOR complex integrity and regulates Akt phosphorylation and substrate specificity. *Cell* **127**, 125–137 (2006).
51. P. Liu, W. Gan, H. Inuzuka, A. S. Lazorchak, D. Gao, O. Arojo, D. Liu, L. Wan, B. Zhai, Y. Yu, M. Yuan, B. Mo Kim, S. Shaik, S. Menon, S. P. Gygi, T. Ho Lee, J. M. Asara, B. D. Manning, J. Blenis, B. Su, W. Wei, Sin1 phosphorylation impairs mTORC2 complex integrity and inhibits downstream Akt signalling to suppress tumorigenesis. *Nat. Cell Biol.* **15**, 1340–1350 (2013).
52. Y. P. Mossé, S. D. Voss, M. S. Lim, D. Rolland, C. G. Minard, E. Fox, Targeting ALK with crizotinib in pediatric anaplastic large cell lymphoma and inflammatory myofibroblastic tumor: A Children's Oncology Group Study. *J. Clin. Oncol.* **35**, 3215–3221 (2017).
53. G. Hrustanovic, T. G. Bivona, RAS signaling in ALK fusion lung cancer. *Small GTPases* **7**, 32–33 (2016).
54. I. Lambertz, C. Kumps, S. Claeys, S. Lindner, A. Beckers, E. Janssens, D. R. Carter, A. Cazes, B. B. Cheung, M. De Mariano, A. De Bondt, S. De Brouwer, O. Delattre, J. Gibbons, I. Janoueix-Lerosey, G. Laureys, C. Liang, G. M. Marchall, M. Porcu, J. Takita, D. Camacho Trujillo, I. Van Den Wyngaert, N. Van Roy, A. Van Goethem, T. Van Maerken, P. Zabrocki, J. Cools, J. H. Schulte, J. Vialard, F. Speleman, K. De Preter, Upregulation of MAPK negative feedback regulators and RET in mutant ALK neuroblastoma: Implications for targeted treatment. *Clin. Cancer Res.* **21**, 3327–3339 (2015).
55. J. Downward, Targeting RAS signalling pathways in cancer therapy. *Nat. Rev. Cancer* **3**, 11–22 (2003).
56. J. A. Engelman, J. Luo, L. C. Cantley, The evolution of phosphatidylinositol 3-kinases as regulators of growth and metabolism. *Nat. Rev. Genet.* **7**, 606–619 (2006).
57. M. C. Mendoza, E. E. Er, J. Blenis, The Ras-ERK and PI3K-mTOR pathways: Cross-talk and compensation. *Trends Biochem. Sci.* **36**, 320–328 (2011).
58. R. B. Corcoran, H. Ebi, A. B. Turke, E. M. Coffee, M. Nishino, A. P. Cogdill, R. D. Brown, P. D. Pelle, D. Dias-Santagata, K. E. Hung, K. T. Flaherty, A. Piris, J. A. Wargo, J. Settleman, M. Mino-Kenudson, J. A. Engelman, EGFR-mediated reactivation of MAPK signaling contributes to insensitivity of *BRAF*-mutant colorectal cancers to RAF inhibition with vemurafenib. *Cancer Discov.* **2**, 227–235 (2012).
59. S. J. Heidorn, C. Milagre, S. Whittaker, A. Nourry, I. Niculescu-Duvas, N. Dhomen, J. Hussain, J. S. Reis-Filho, C. J. Springer, C. Pritchard, R. Marais, Kinase-dead BRAF and oncogenic RAS cooperate to drive tumor progression through CRAF. *Cell* **140**, 209–221 (2010).
60. B. Sanchez-Laorden, A. Viros, M. R. Girotti, M. Pedersen, G. Saturno, A. Zambon, D. Niculescu-Duvaz, S. Turajlic, A. Hayes, M. Gore, J. Larkin, P. Lorigan, M. Cook, C. Springer, R. Marais, BRAF inhibitors induce metastasis in RAS mutant or inhibitor-resistant melanoma cells by reactivating MEK and ERK signaling. *Sci. Signal.* **7**, ra30 (2014).
61. H. P. Soares, M. Ming, M. Mellon, S. H. Young, L. Han, J. Sinnet-Smith, E. Rozengurt, Dual PI3K/mTOR inhibitors induce rapid overactivation of the MEK/ERK pathway in human pancreatic cancer cells through suppression of mTORC2. *Mol. Cancer Ther.* **14**, 1014–1023 (2015).
62. A. B. Turke, Y. Song, C. Costa, R. Cook, C. L. Arteaga, J. M. Asara, J. A. Engelman, MEK inhibition leads to PI3K/AKT activation by relieving a negative feedback on ERBB receptors. *Cancer Res.* **72**, 3228–3237 (2012).
63. S.-M. Chen, C.-L. Guo, J.-J. Shi, Y.-C. Xu, Y. Chen, Y.-Y. Shen, Y. Su, J. Ding, L.-H. Meng, HSP90 inhibitor AUY922 abrogates up-regulation of RTKs by mTOR inhibitor AZD8055 and potentiates its antiproliferative activity in human breast cancer. *Int. J. Cancer* **135**, 2462–2474 (2014).
64. L. Bar-Peled, D. M. Sabatini, Regulation of mTORC1 by amino acids. *Trends Cell Biol.* **24**, 400–406 (2014).

65. M. Breuleux, M. Klopfenstein, C. Stephan, C. A. Doughty, L. Barys, S.-M. Maira, D. Kwiatkowski, H. A. Lane, Increased AKT S473 phosphorylation after mTORC1 inhibition is rictor dependent and does not predict tumor cell response to PI3K/mTOR inhibition. *Mol. Cancer Ther.* **8**, 742–753 (2009).
66. M. Laplante, D. M. Sabatini, mTOR signaling in growth control and disease. *Cell* **149**, 274–293 (2012).
67. G. Yang, D. S. Murashige, S. J. Humphrey, D. E. James, A positive feedback loop between Akt and mTORC2 via SIN1 phosphorylation. *Cell Rep.* **12**, 937–943 (2015).
68. S. J. Humphrey, D. E. James, M. Mann, Protein phosphorylation: A major switch mechanism for metabolic regulation. *Trends Endocrinol. Metab.* **26**, 676–687 (2015).
69. C. C. Dibble, J. M. Asara, B. D. Manning, Characterization of Rictor phosphorylation sites reveals direct regulation of mTOR complex 2 by S6K1. *Mol. Cell. Biol.* **29**, 5657–5670 (2009).
70. S. Mohlin, A. Hamidian, K. von Stedingk, E. Bridges, C. Wigerup, D. Bexell, S. Påhlman, PI3K–mTORC2 but not PI3K–mTORC1 regulates transcription of HIF2A/EPAS1 and vascularization in neuroblastoma. *Cancer Res.* **75**, 4617–4628 (2015).
71. D. Boulbes, C.-H. Chen, T. Shaikenov, N. K. Agarwal, T. R. Peterson, T. A. Addona, H. Keshishian, S. A. Carr, M. A. Magnuson, D. M. Sabatini, D. D. Sarbassov, Rictor phosphorylation on the Thr-1135 site does not require mammalian target of rapamycin complex 2. *Mol. Cancer Res.* **8**, 896–906 (2010).
72. C. Treins, P. H. Warne, M. A. Magnuson, M. Pende, J. Downward, Rictor is a novel target of p70 S6 kinase-1. *Oncogene* **29**, 1003–1016 (2010).
73. A. C. Wood, K. Krytska, H. T. Ryles, N. R. Infarinato, R. Sano, T. D. Hansel, L. S. Hart, F. J. King, T. R. Smith, E. Ainscow, K. B. Grandinetti, T. Tuntland, S. Kim, G. Caponigro, Y. Qun He, S. Krupa, N. Li, J. L. Harris, Y. P. Mossé, Dual *ALK* and *CDK4/6* inhibition demonstrates synergy against neuroblastoma. *Clin. Cancer Res.* **23**, 2856–2868 (2016).
74. H. Carén, H. Kryh, M. Nethander, R.-M. Sjöberg, C. Träger, S. Nilsson, J. Abrahamsson, P. Kogner, T. Martinsson, High-risk neuroblastoma tumors with 11q-deletion display a poor prognostic, chromosome instability phenotype with later onset. *Proc. Natl. Acad. Sci. U.S.A.* **107**, 4323–4328 (2010).
75. S. Fransson, M. Hansson, K. Ruuth, A. Djos, A. Berbegall, N. Javanmardi, J. Abrahamsson, R. H. Palmer, R. Noguera, B. Hallberg, P. Kogner, T. Martinsson, Intragenic anaplastic lymphoma kinase (*ALK*) rearrangements: Translocations as a novel mechanism of *ALK* activation in neuroblastoma tumors. *Genes Chromosomes Cancer* **54**, 99–109 (2015).
76. T. C. Chou, P. Talalay, Quantitative analysis of dose-effect relationships: The combined effects of multiple drugs or enzyme inhibitors. *Adv. Enzyme Regul.* **22**, 27–55 (1984).

Acknowledgments: We thank S. Nilsson (Department of Mathematical Sciences, Chalmers University of Technology, Sweden) for the help with the statistical analyses. The H3122 and DFCI032 cell lines were gifts from R. George and P. Jänne (Dana-Farber Cancer Institute). **Funding:** This work was supported by the Swedish Cancer Society (15/391 to R.H.P.; 15/775 to B.H.; 15/827 to T.M.), the Swedish Childhood Cancer Foundation (2015-0096 to R.H.P.; 2015-80 and 2014-150 to B.H.; 2013-102 to T.M.), the Swedish Research Council (2015-04466 to R.H.P.; BH 521-2012-2831 and 521-2014-3031 to T.M.), the Göran Gustafsson Foundation (to R.H.P.), and an Stiftelsen för Strategisk Forskning Programme Grant (RB13-0204 to R.H.P., T.M., and B.H.). **Author contributions:** G.U. and J.G. carried out all the cell and biochemical analyses. D.E.G. and D.C.-M. executed the animal experiments. N.J., A.D., and T.M. investigated and verified all the cell lines used in the study. R.H.P. and B.H. supervised the project and wrote the manuscript together with G.U. **Competing interests:** The authors declare that they have no competing interests. **Data and materials availability:** The CLB-BAR, CLB-GE, CLB-GA, and CLB-PE cell lines used in this study are under an MTA agreement with the Center Léon Bérard laboratory (Lyon, France).

Submitted 11 January 2017
Accepted 31 October 2017
Published 28 November 2017
10.1126/scisignal.aam7550

Citation: G. Umapathy, J. Guan, D. E. Gustafsson, N. Javanmardi, D. Cervantes-Madrid, A. Djos, T. Martinsson, R. H. Palmer, B. Hallberg, MEK inhibitor trametinib does not prevent the growth of anaplastic lymphoma kinase (ALK)–addicted neuroblastomas. *Sci. Signal.* **10**, eaam7550 (2017).

Science Signaling

MEK inhibitor trametinib does not prevent the growth of anaplastic lymphoma kinase (ALK)–addicted neuroblastomas

Ganesh Umapathy, Jikui Guan, Dan E. Gustafsson, Niloufar Javanmardi, Diana Cervantes-Madrid, Anna Djos, Tommy Martinsson, Ruth H. Palmer and Bengt Hallberg

Sci. Signal. **10** (507), eaam7550.
DOI: 10.1126/scisignal.aam7550

Feedback signaling complicates treatment

Trametinib, an inhibitor of the kinase MEK, is clinically approved to treat patients with various types of cancers. Because some cases, particularly relapses, of neuroblastoma often display increased activation of the RAS-MAPK pathway, which includes MEK, trametinib is proposed as a rational combination strategy for treating ALK-addicted neuroblastomas. However, Umapathy *et al*. found that this may not be effective. The authors evaluated various ALK-addicted and RAS-mutant neuroblastoma cell lines and EML4-ALK–positive NSCLC cell lines in mice and found that trametinib did not inhibit growth. Rather, MEK pathway inhibition by trametinib induced a prosurvival feedback signal mediated by AKT and mTORC2. Thus, although it seems to be a rational therapeutic target, inhibiting the RAS-MAPK pathway would likely not benefit patients with ALK-addicted neuroblastoma.